Supplementary Information for:
On the structure of hybrid water-in-salt electrolytes

Raúl Lois-Cuns[a,b,‡], Antía Santiago-Alonso[a,b,c,‡], Martín Otero-Lema[a,b], Juan J. Parajó[a,b], Josefa Salgado[a,b], Hadrián Montes-Campos[*,a,b], Trinidad Méndez-Morales[*,a,b], and Luis M. Varela[a,b]

[a] *Grupo de Nanomateriais, Fotónica e Materia Branda, Departamento de Física de Partículas - Universidade de Santiago de Compostela, Campus Vida s/n E-15782, Santiago de Compostela, Spain. E-mail: hadrian.montes@usc.es, trinidad.mendez@usc.es*
[b] *Instituto de Materiais (iMATUS) - Universidade de Santiago de Compostela, Avenida do Mestre Mateo 25 E-15782, Santiago de Compostela, Spain.*
[c] *ABCR LABORATORIOS, Lg. Vilapouca (PG Industrial) E-36550, Forcarei, Spain.*

Materials and methods

Experimental mixtures

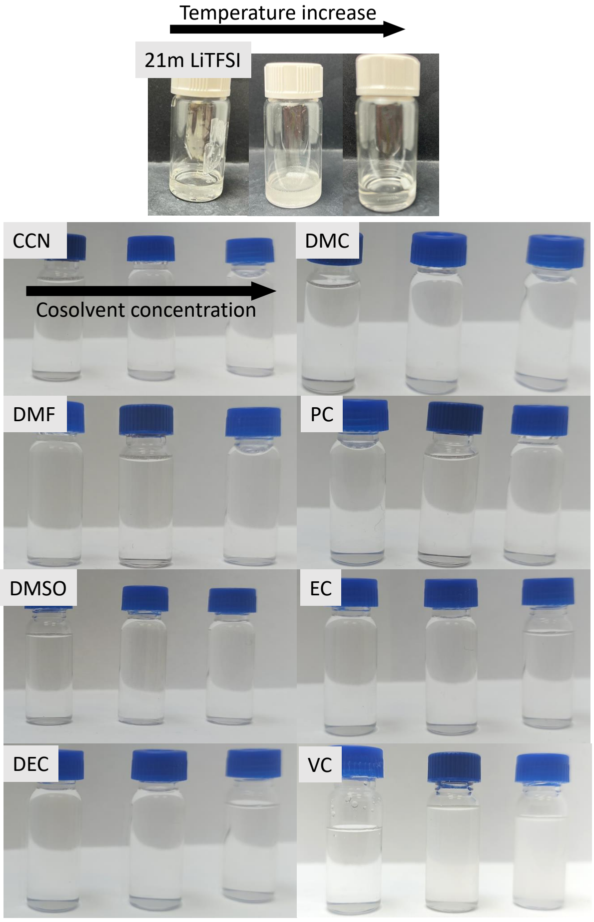

Figure S1 Pictures of all the experimental mixtures after one month. All the samples were kept at room temperature. Notably, the melting point of pure WiS is very close to room temperature, allowing for the formation of crystals upon deposition. Once it absorbs a small amount of heat from the environment, for exampling by handling the mixture, WiS melts completely. This process could be observed at the top of the figure as the temperature is slightly increased.

[‡] These authors contributed equally to this work.

Simulation parameters

When selecting a suitable water model, various models were evaluated to determine which one most accurately replicates the experimental properties of the 21 m WiS electrolyte. The water models tested included TIP3P[1], TIP4P[1], TIP5P[2], SPC[3], SPC/E[3], and OPC3[4]. Ion charges were scaled by a factor 0.8. Experimental measurements of density and diffusion coefficients of the species of the system were chosen as the key parameters for comparison. Table S1 presents the density results, while Fig. S2 illustrates the comparison of diffusion coefficients.

Water model	Density [g/cm^3]
TIP3P	1701.72
TIP4P	1731.16
TIP5P	1780.94
SPC	1707.20
SPC/E	1717.95
OPC3	1721.57
Experimental	1724.00[5]

Table S1 Density values for 21 m LiTFSI WiS electrolyte for different water models.

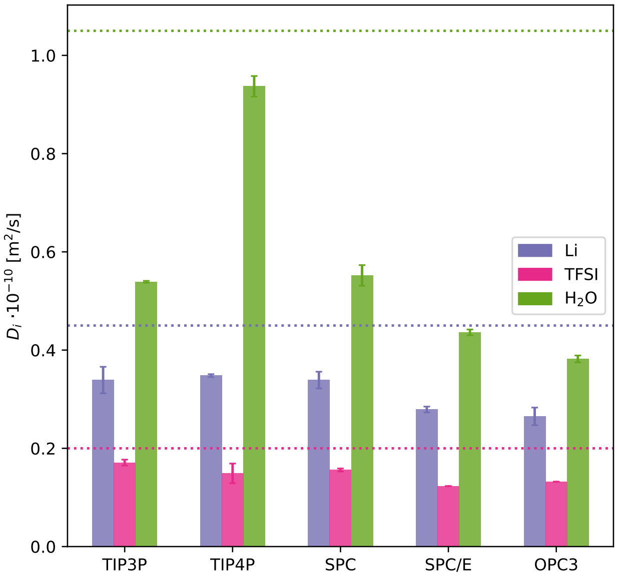

Figure S2 Diffusion coefficients for the cation, anion and water molecules for the different models. Dotted lines represent experimental values used for comparison[6].

The parametrization for the ACN molecule is shown in Table S2.

	m [a.u]	q [e]	σ [Å]	ε [kJ/mol]
C1	12.0110	-0.080	3.3	0.276144
C2	12.0110	0.460	3.3	0.276144
N3	14.0067	-0.560	3.2	0.711280
H	1.00800	0.060	2.5	0.062760

Table S2 Parameters for the atoms in the ACN molecule. C2 denotes the carbon bonded to the nitrogen atom, while the C1 carbon atom is bonded to three identical hydrogen atoms, as well as to the C1 carbon.

Results and discussion

X-ray structure factor

Taking atomic form factors into account, the X-ray structure factor is given by

$$S^X(q) = \frac{1}{\sum_\alpha x_\alpha f_\alpha^2(q)} \sum_\alpha^n \sum_\beta^n f_\alpha(q) f_\beta(q) S_{\alpha\beta}(q), \tag{1}$$

where $S_{\alpha\beta}$ is the partial structure factor between atomic species α and β, x_α is the molar fraction of the element α and f_α its form factor for X-ray scattering. The atomic form factors were taken from the International Tables for Crystallography[7]. The X-ray structure factors for all systems can be found in Fig. S3.

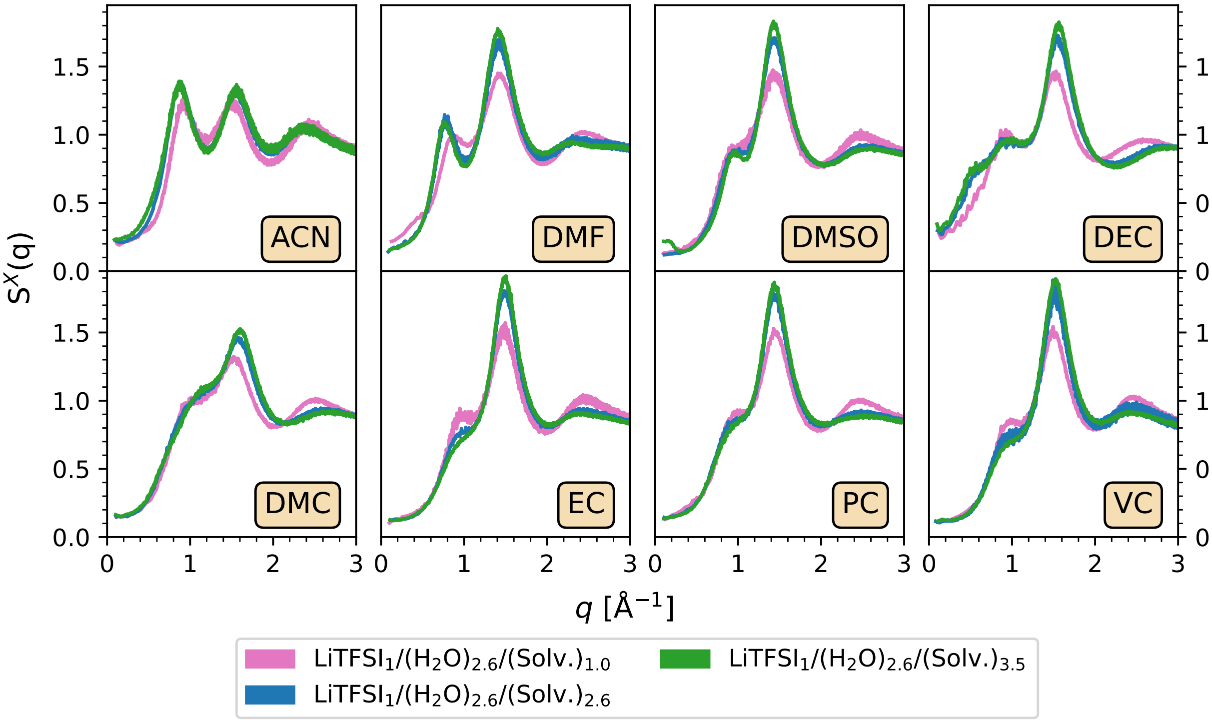

Figure S3 Computational X-ray structure factors $S^X(q)$ as a function of the wave vector modulus q for the different concentrations of the co-solvents.

Partial structure factors

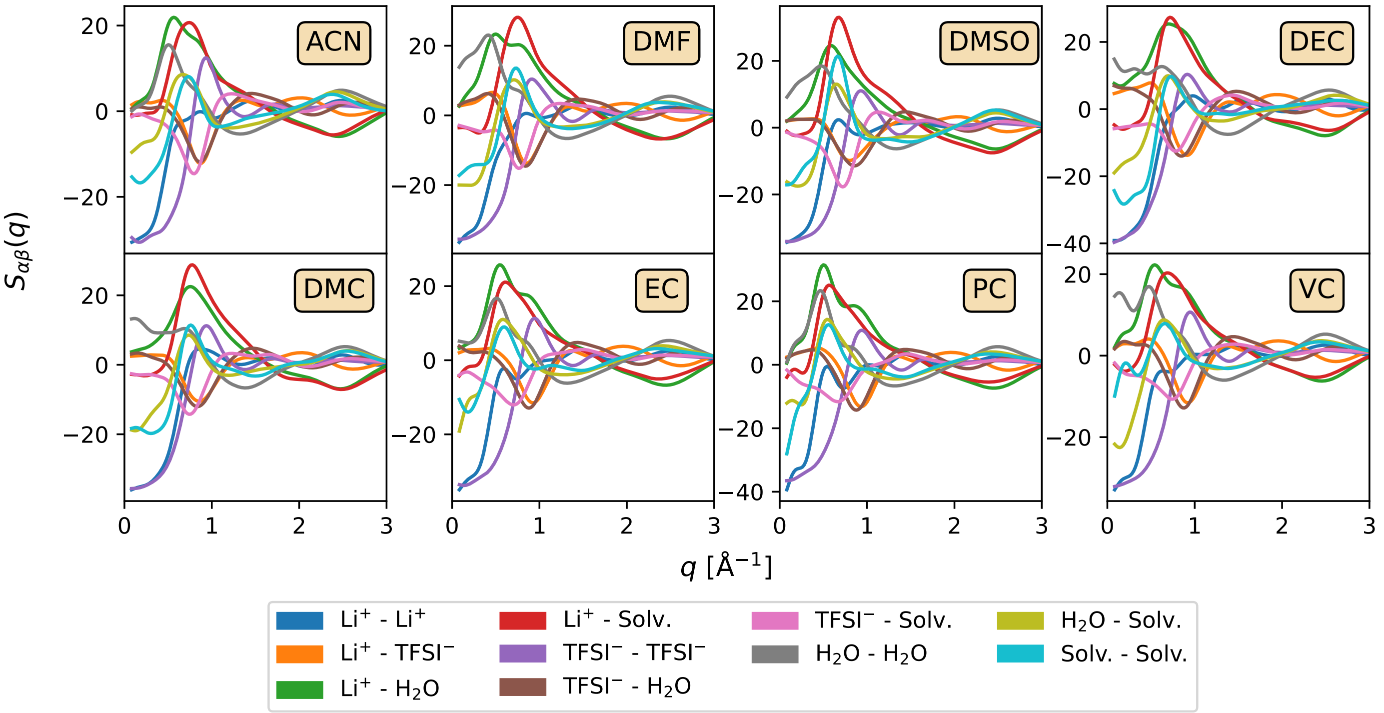

Figure S4 Partial structure factors $S_{\alpha\beta}(q)$ as a function of the wave vector modulus q for the LiTFSI$_1$/(H$_2$O)$_{2.6}$/(Solv)$_{1.0}$ systems.

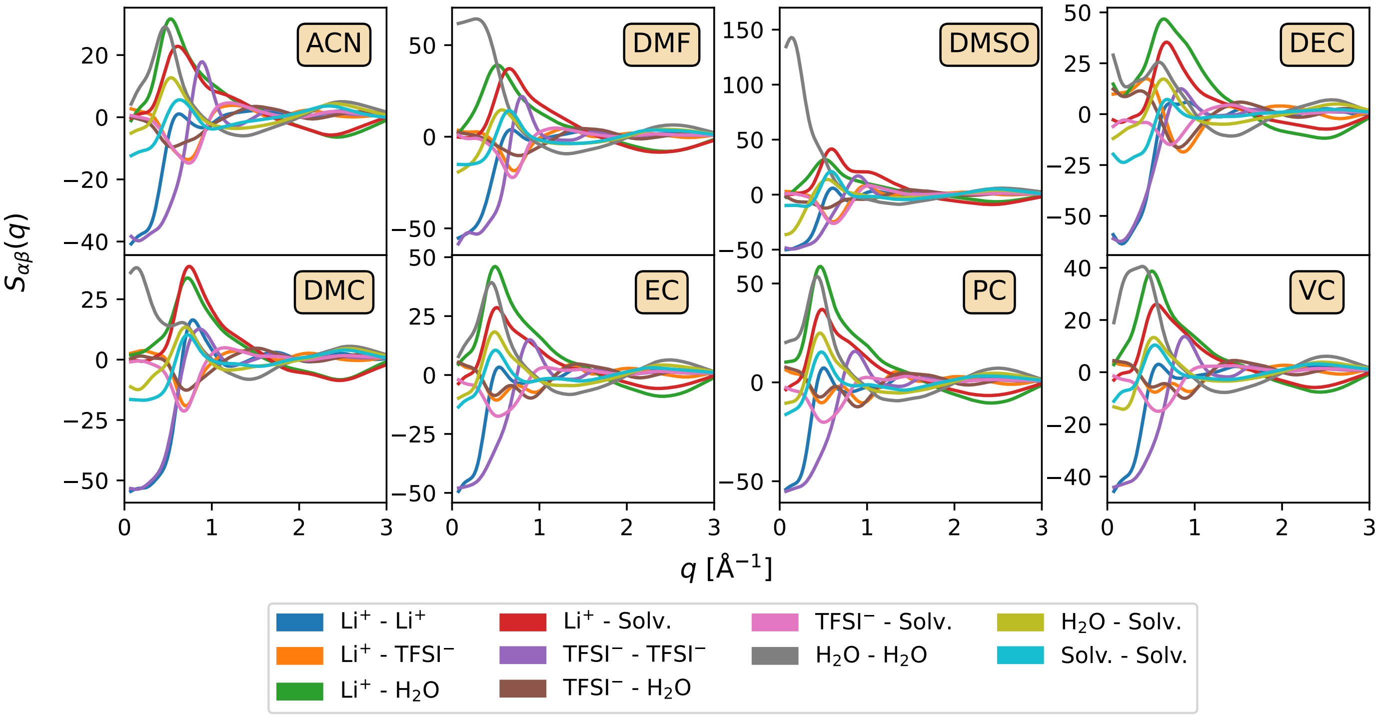

Figure S5 Partial structure factors $S_{\alpha\beta}(q)$ as a function of the wave vector modulus q for the LiTFSI$_1$/(H$_2$O)$_{2.6}$/(Solv)$_{2.6}$ systems.

Water cluster population

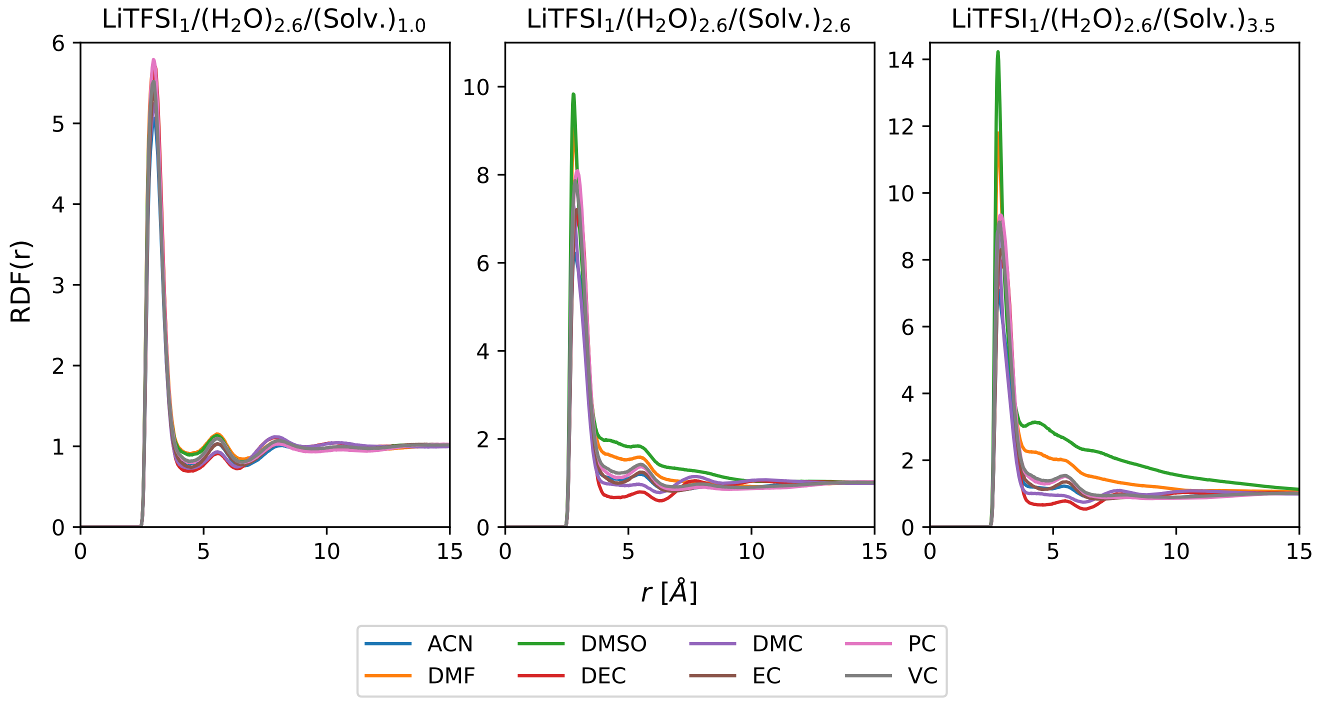

Figure S6 Radial distribution functions between the oxygen atom of water molecules for the different co-solvent mole fractions (increasing from top to bottom).

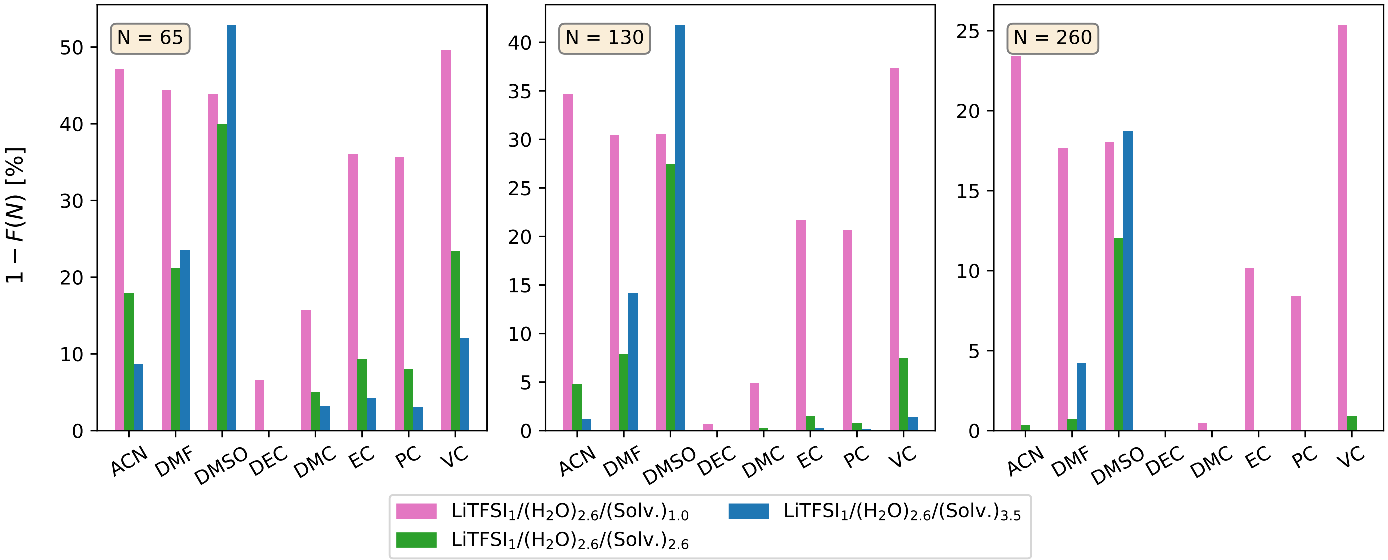

Figure S7 Fraction of water molecules that belong to a cluster with at least N water molecules, for different values of N. These values represent 2.5%, 5.0% and 10.0% of the total water molecules inside the simulation boxes.

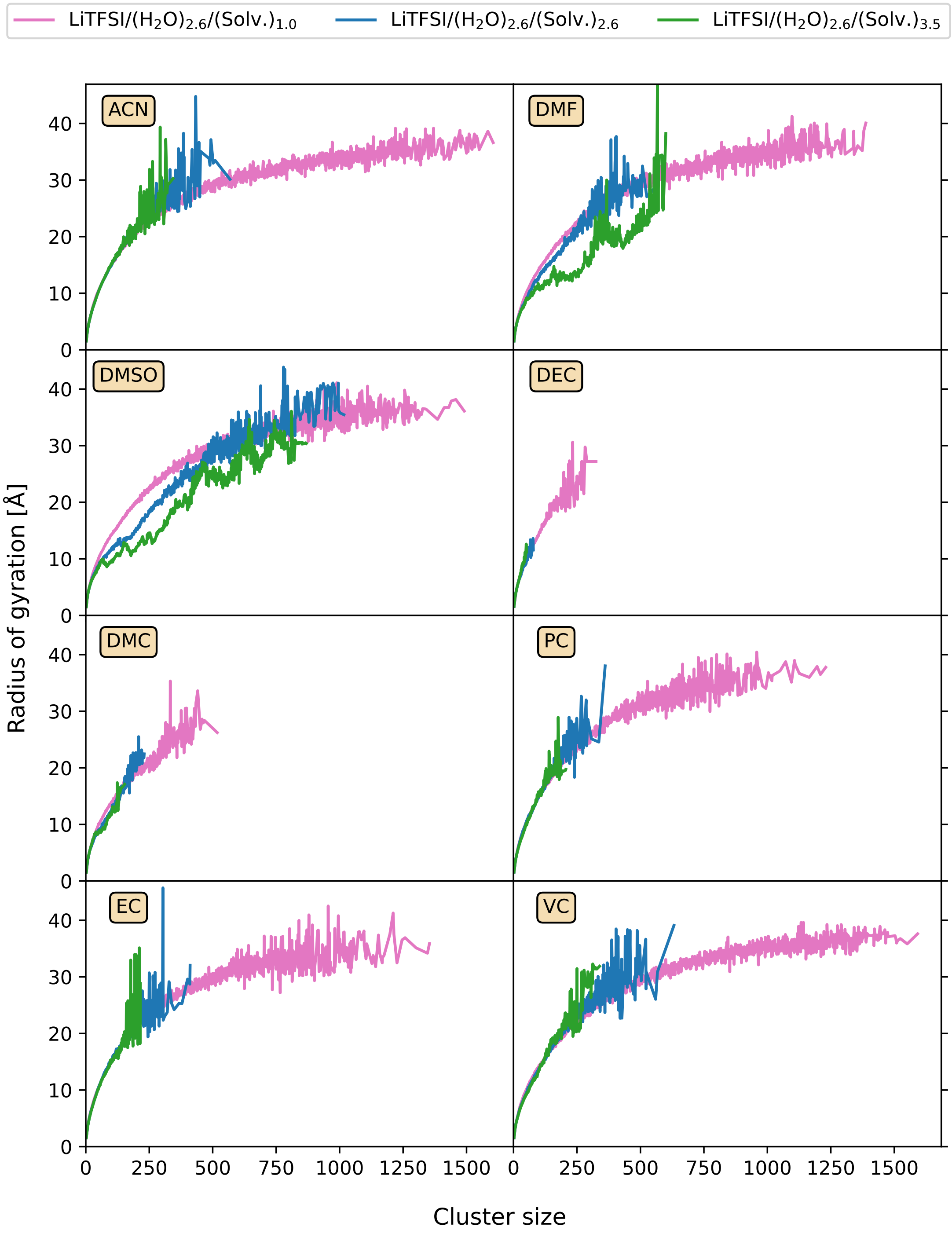

Figure S8 Radius of gyration for the different cluster size and systems.

Nuclear Magnetic Resonance

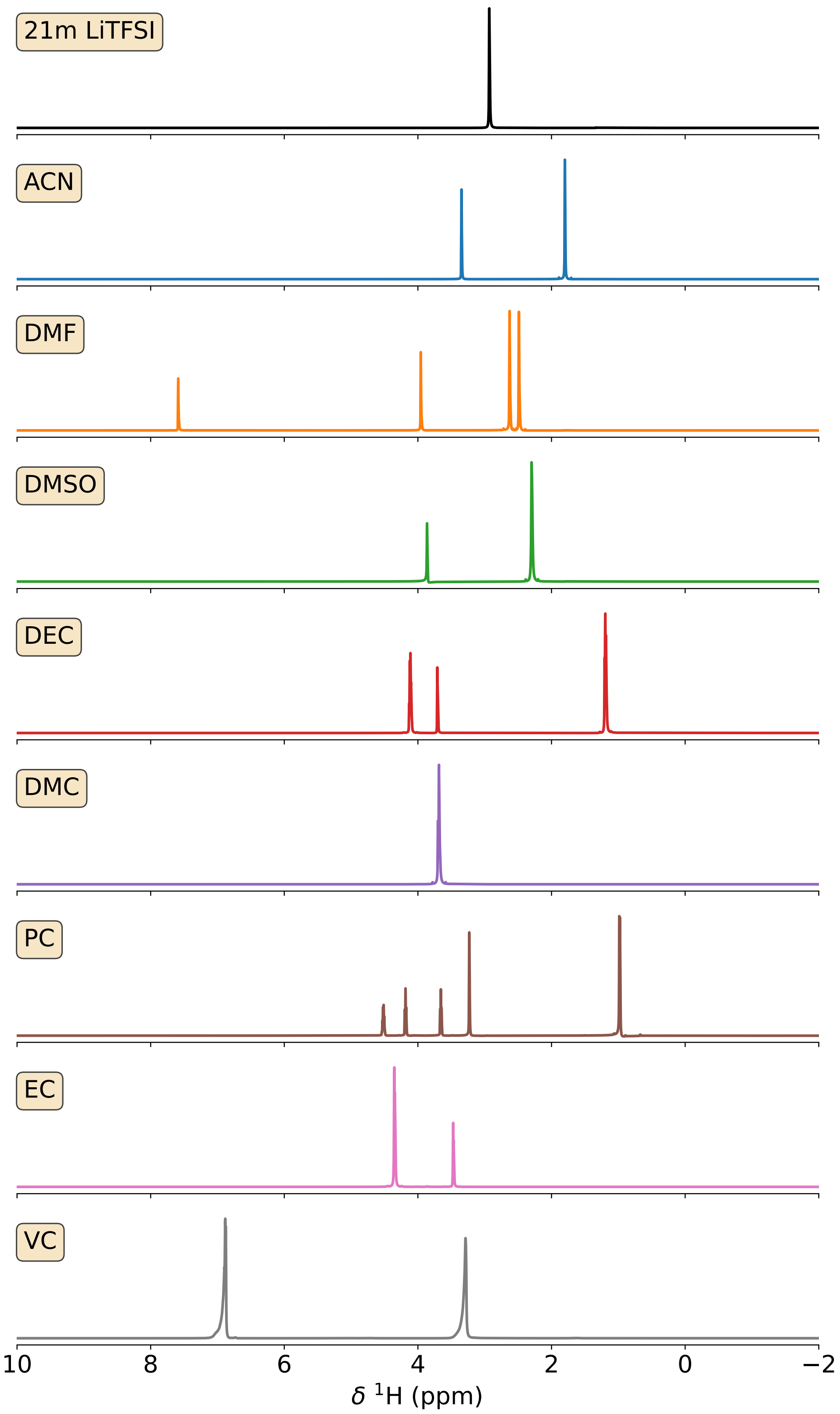

Figure S9 Normalized NMR measurements spectra of $LiTFSI_1/(H_2O)_{2.6}/(Solv)_{3.5}$ electrolytes showing the ^{1}H chemical shift.

Chemical shift models

Two different models are used to compare the $\delta^1 H$ chemical shift of water molecules with the fractions of water involved in Li^+ coordination (and, therefore, the "free water fraction"). The first one is a two contribution model described by:

$$\delta^1 H = \delta^1 H_{WiS} \cdot f + \delta^1 H_w \cdot (1-f) = 4.7 \cdot f + 2.93 \cdot (1-f) \tag{2}$$

where f is the fraction of water molecules that are found in the first solvation shell of Li^+ cations and $\delta^1 H_{w/WiS}$ are the experimental values corresponding to the ^1H chemical shift of water molecules for the pure-water/WiS systems.

A three contribution model that takes into account the cosolvent-water interactions is also considered:

$$\delta^1 H = \delta^1 H_{WiS} \cdot f + \delta^1 H_w \cdot f' + \delta^1 H_{sw} \cdot (1-f-f') \tag{3}$$

where now f', which represents the free water fraction, corresponds to the water molecules that have more water molecules in their solvation shell than cosolvent molecules and $\delta^1 H_{sw}$ represents the shift of water molecules in cosolvent media.

To compute the value of $\delta^1 H_{sw}$, density functional theory (DFT) simulations were carried out. Different complexes composed by one water molecule surrounded by four cosolvent molecules, whose geometries were optimized, were used to compute the NMR spectra by means of the gauge-independent atomic orbital (GIAO) method. To properly take into account the solvent effects, the polarizable continuum model (PCM) was used. The static dielectric constants and optical dielectric constants for the cosolvent used during these simulations are listed in the table below.

System	ε_r	n^2
ACN	36.64	1.800687
DMF	38.25	2.046330
DMSO	47.24	2.185371
DEC	2.820	1.915456
DMC	3.087	1.876078
PC	66.14	2.013277
EC	89.78	2.001659
VC	127	2.019241
TMS	80.1	1.846065

Table S3 Static dielectric constant, ε_r, and, optical dielectric constant, n^2, for the different solvents used during DFT simulations.

All calculations were performed using Gaussian 16[8]. The initial geometries were optimized at the B3LYP/6-311G(d,p) level of theory, including Grimme's D3 empirical dispersion correction with Becke–Johnson damping[9]. For the NMR calculations, the WP04 functional was employed, as it is specifically parameterized for accurate proton chemical shift prediction[10]. Additionally, the extended 6-311++G(2d,p) basis set was used to improve the description of electronic environments. For the optimization procedure the converge option was set to Tight and Ultrafine was selected as the integradion grid. For the computation of the shift of the ^1H spectra, tetramethylsilane (TMS) was used as reference. Its spectra was computed using the same procedure described above but using only two TMS molecules as input for the computations.

In order to compute the water fractions, for each simulation frame an undirected graph is built, where each node represents metal cations, water molecules or cosolvent molecules. One water molecule node is connected to any of the other nodes if any of the atoms of one molecule is at a distance of 2.7 Å (which correspond to the first minimum of the minimum-distance distribution functions of water molecules depicted in Fig. S10). From that the different water fractions can be computed looking at the connections of the graph. A water molecule is considered to contribute to the fraction of water molecules that are in the first solvation shell of Li^+ if at least one cation is connected to it. Then, a water molecule contributes to f' if there are more water molecules connected to it than cosolvent molecules.

Minimum-distance distribution functions of H_2O molecules

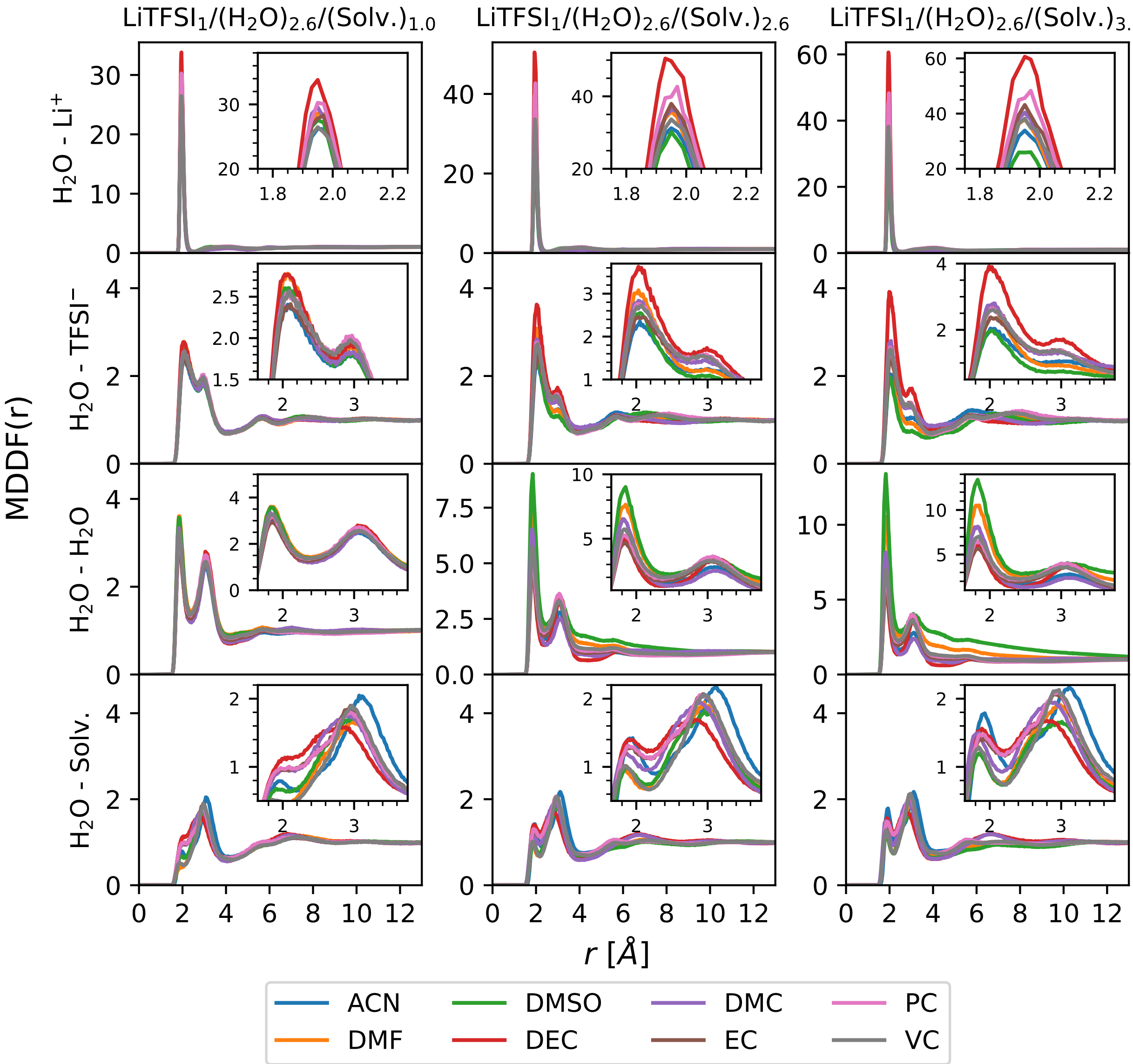

Figure S10 Minimum-distance distribution functions (MDDFs) between H_2O molecules and (from top to bottom) Li^+ cations, $TFSI^-$ anions, H_2O molecules and co-solvent molecules for the different concentrations (increasing from left to right).

Notes and references

[1] W. L. Jorgensen, J. Chandrasekhar, J. D. Madura, R. W. Impey and M. L. Klein, *J. Chem. Phys.*, 1983, **79**, 926–935.

[2] M. W. Mahoney and W. L. Jorgensen, *J. Chem. Phys.*, 2000, **112**, 8910–8922.

[3] H. J. C. Berendsen, J. R. Grigera and T. P. Straatsma, *J. Phys. Chem-Us*, 1987, **91**, 6269–6271.

[4] S. Izadi and A. V. Onufriev, *J. Chem. Phys.*, 2016, **145**, 074501.

[5] Y. Zhang, N. H. Lewis, J. Mars, G. Wan, N. J. Weadock, C. J. Takacs, M. R. Lukatskaya, H.-G. Steinrück, M. F. Toney, A. Tokmakoff *et al.*, *J. Phys. Chem. B*, 2021, **125**, 4501–4513.

[6] Y. Zhang and E. J. Maginn, *J. Phys. Chem. B*, 2021, **125**, 13246–13254.

[7] P. Brown, A. Fox, E. Maslen, M. O'keefe and B. Willis, *International Tables for Crystallography C*, 2006, **C**, 554–595.

[8] M. J. Frisch, G. W. Trucks, H. B. Schlegel, G. E. Scuseria, M. A. Robb, J. R. Cheeseman, G. Scalmani, V. Barone, G. A. Petersson, H. Nakatsuji, X. Li, M. Caricato, A. V. Marenich, J. Bloino, B. G. Janesko, R. Gomperts, B. Mennucci, H. P. Hratchian, J. V. Ortiz, A. F. Izmaylov, J. L. Sonnenberg, D. Williams-Young, F. Ding, F. Lipparini, F. Egidi, J. Goings, B. Peng, A. Petrone, T. Henderson, D. Ranasinghe, V. G. Zakrzewski, J. Gao, N. Rega, G. Zheng, W. Liang, M. Hada, M. Ehara, K. Toyota, R. Fukuda, J. Hasegawa, M. Ishida, T. Nakajima, Y. Honda, O. Kitao, H. Nakai, T. Vreven, K. Throssell, J. A. Montgomery, Jr., J. E. Peralta, F. Ogliaro, M. J. Bearpark, J. J. Heyd, E. N. Brothers, K. N. Kudin, V. N. Staroverov, T. A. Keith, R. Kobayashi, J. Normand, K. Raghavachari, A. P. Rendell, J. C. Burant, S. S. Iyengar, J. Tomasi, M. Cossi, J. M. Millam, M. Klene, C. Adamo, R. Cammi, J. W. Ochterski, R. L. Martin, K. Morokuma, O. Farkas, J. B. Foresman and D. J. Fox, *Gaussian∼16 Revision C.01*, 2016, Gaussian Inc. Wallingford CT.

[9] S. Grimme, S. Ehrlich and L. Goerigk, *Journal of computational chemistry*, 2011, **32**, 1456–1465.

[10] K. W. Wiitala, T. R. Hoye and C. J. Cramer, *Journal of Chemical Theory and Computation*, 2006, **2**, 1085–1092.